EXPERIMENTAL INVESTIGATION AND CFD SIMULATION OF HORIZONTAL STRATIFIED TWO-PHASE FLOW PHENOMENA

Christophe Vallée, Thomas Höhne, Horst-Michael Prasser, Tobias Sühnel
Forschungszentrum Rossendorf e.V., Dresden, Germany

Abstract

For the investigation of stratified two-phase flow, two horizontal channels with rectangular cross-section were built at *Forschungszentrum Rossendorf*. The channels allow the investigation of air/water co-current flows, especially the slug behaviour, at atmospheric pressure and room temperature. The test-sections are made of acrylic glass, so that optical techniques, like high-speed video observation or particle image velocimetry (PIV), can be applied for measurements. The rectangular cross-section was chosen to provide better observation possibilities. Moreover, dynamic pressure measurements were performed and synchronised with the high-speed camera system.

CFD post test simulations of stratified flows were performed using the code *ANSYS CFX*. The Euler-Euler two fluid model with the free surface option was applied on grids of minimum $4 \cdot 10^5$ control volumes. The turbulence was modelled separately for each phase using the k-ω based shear stress transport (SST) turbulence model. The results compare very well in terms of slug formation, velocity, and breaking. The qualitative agreement between calculation and experiment is encouraging and shows that CFD can be a useful tool in studying horizontal two-phase flow.

Introduction

Slug flow as a multiphase flow regime can occur in the main cooling lines of pressurized water reactors, for instance after a small break Loss of Coolant Accident (SB-LOCA), and also in other fields, like chemical plants or oil pipelines. The slug flow regime is usually characterized by an acceleration of the gaseous phase and by the transition of fast liquid slugs, which carry a significant amount of liquid with high kinetic energy. It is potentially hazardous to the structure of the system due to the strong oscillating pressure levels formed behind the liquid slugs as well as the mechanical momentum of the slugs.

For the experimental investigation of air/water flows, two horizontal channels with rectangular cross-section were built at *Forschungszentrum Rossendorf*. The first channel, allowing co- and counter-current flows, was used for preliminary studies. As some uncertainties were noticed at the inlet of the test-section, the HAWAC (Horizontal Air/Water Channel) dedicated to co-current flows was built. Its improved inlet device provides defined inlet boundary conditions. Both channels allow in particular the study of air/water slug flow under atmospheric pressure.

Parallel to the experiments, CFD calculations were carried out. The aim of the numerical simulations is the validation of prediction of the slug flow with the existing multiphase flow models built in the commercial code *ANSYS CFX*. Further it is of interest to prove the understanding of the general fluid dynamic mechanism leading to slug flow and to identify the critical parameters affecting the main slug flow parameters (like e.g. slug length, frequency and propagation velocity; pressure drop).

1. Previous modelling of slug flow

According to Manfield (2000), only few attempts using CFD to study slug flow have been made. He simulated a single, isolated liquid slug using a three-dimensional CFD Volume-of-Fluid (VOF) method. Three models of varying complexity were developed: a simulation of the tail of an “infinitely long” slug, a model of short slug whose front is represented by a solid barrier and a simulation of a slug front as a gas-liquid interface.

Other groups have also reported studies of slug flow using CFD. Mao and Dukler (1991) wrote a dedicated CFD programme to simulate the liquid flow around a Taylor bubble in vertical flow. Pan (1996) reported that this was limited in ability and flexibility. Issa and Tang (1990) used a similar approach, also for vertical flow. Moe (1992) simulated the propagation of elongated bubbles in channels initially filled with liquid, closed at one end and open to the atmosphere at the other. Moe also simulated the motion of a single bubble in a pipe containing stagnant liquid, but did not extend this to systems with a net liquid flow. Ubbink (1997) included a case study of the shape and rise velocity of Taylor bubbles in vertical flow as part of his general investigation into the modelling of gas-liquid interfaces. He used a moving-wall boundary condition and simulated a “wedge” of axisymmetric vertical flow. The initial position of the interface was taken from experimental observations and Ubbink simulated the development of the interface shape with time.

Recently, Anglart and Podowski (2002) investigated the fluid mechanics of Taylor bubbles and slug flows in vertical, circular channels using detailed, three-dimensional CFD simulations. The Volume-of-Fluid model with the interface-sharpening algorithm, implemented in the commercial *CFX-4* code, was used to predict shape and velocity of Taylor bubbles moving along a vertical channel. Several cases were investigated, including both a single Taylor bubble and a train of bubbles rising in

water. The computer simulations that were performed revealed the importance of properly modelling the three-dimensional nature of phenomena governing the motion of Taylor bubbles.

Lun et al. (1996) used the commercial CFD programme FIDAP to simulate the growth of a wave on the interface of two immiscible fluids with different properties in horizontal stratified gas-liquid flow. The method used to simulate the liquid surface was not described. A coarse two-dimensional grid was developed to represent the flow domain. Significant numerical instabilities during the calculation led to convergence difficulties. These were ascribed to the coarseness of the meshes. Results show the growth of a wave until it completely broaches the pipe and thus initiates slug flow. However, it seems unlikely that the simulated wave growth was completely unbiased by the numerical instabilities.

A three-dimensional slug flow study has been performed by Ujang (2003) for the movement of large Taylor bubbles in a downward inclined pipe. The free surface simulation was conducted using a moving wall boundary. By adjusting the wall speed in accordance with the Taylor bubble rise velocity, the bubble front could be artificially frozen in the computational domain and detailed studies on the formation of the bubble front could be carried out. Close agreement was obtained with air-water experimental data in a 1-inch diameter pipe for a downward angle of -15° and for different fluid velocities.

A systematic study of numerical simulation of slug flow in horizontal pipes using *CFX-5* was carried out by Frank (2003). It was shown that the formation of the slug flow regime strongly depends on the wall friction of the liquid phase. In simulations using inlet/outlet boundary conditions it was found, that the formation of slug flow regimes strongly depends on the agitation or perturbation of the inlet boundary conditions. Furthermore Frank showed that the length of the computational domain plays an important role in slug formation.

Experimental data was delivered by Woods and Hanratty (1999) for a horizontal pipeline with a diameter of 76.3 mm and a length of 20 m. The Perspex pipe segments make it possible to film the flow. Further, liquid holdup and dynamic pressure were measured. Similar experiments were performed by Soleimani and Hanratty (2003) for a 18.3 m long pipe of 25.4 mm diameter.

Nevertheless, the direct comparison between CFD calculations and measurements of the slug generation mechanisms and its propagation in horizontal pipes was not analysed. The recent improvements of the multiphase flow modelling in the *ANSYS CFX* code make it now possible to simulate in detail these mechanisms. In order to validate the implemented models, high-resolution measurement data is needed in time and also in space. Thanks to the optical access of the test channels built at *Forschungszentrum Rossendorf*, it is possible to study detailed local stratified air/water flow phenomena. These experimental results give an important input for two-phase flow CFD model validation (i.e. interfacial momentum transfer, turbulent profiles of each phase).

2. CFD model with time-dependent inlet boundary conditions for slug generation in a short channel

2.1 The horizontal channel with a separator at the inlet

Experiments were carried out at a horizontal duct mounted between two separators (Fig. 2.1). This configuration allows both co-current and counter-current flow experiments. The two-meter long acrylic glass test section has a rectangular cross-section (height x width: 250 x 50 mm²). A jet pump is

driving the water flow, while the air is being injected at the top of one of the separators depending on the type of experiment (co-current or counter-current flow).

The rectangular cross-section was chosen for its optimal optical access in order to observe the flow structure from the side of the duct. A high-speed video camera as well as a PIV-system were used for this purpose. For dynamic pressure measurements, piezoelectric transducers with a rise time of 2 µs were mounted on top of the duct and were synchronised with the high-speed video camera. A dynamic liquid level measurement and an analysis of the slug propagation were achieved by an evaluation of high-speed camera image sequences, both with a time resolution of 100 Hz.

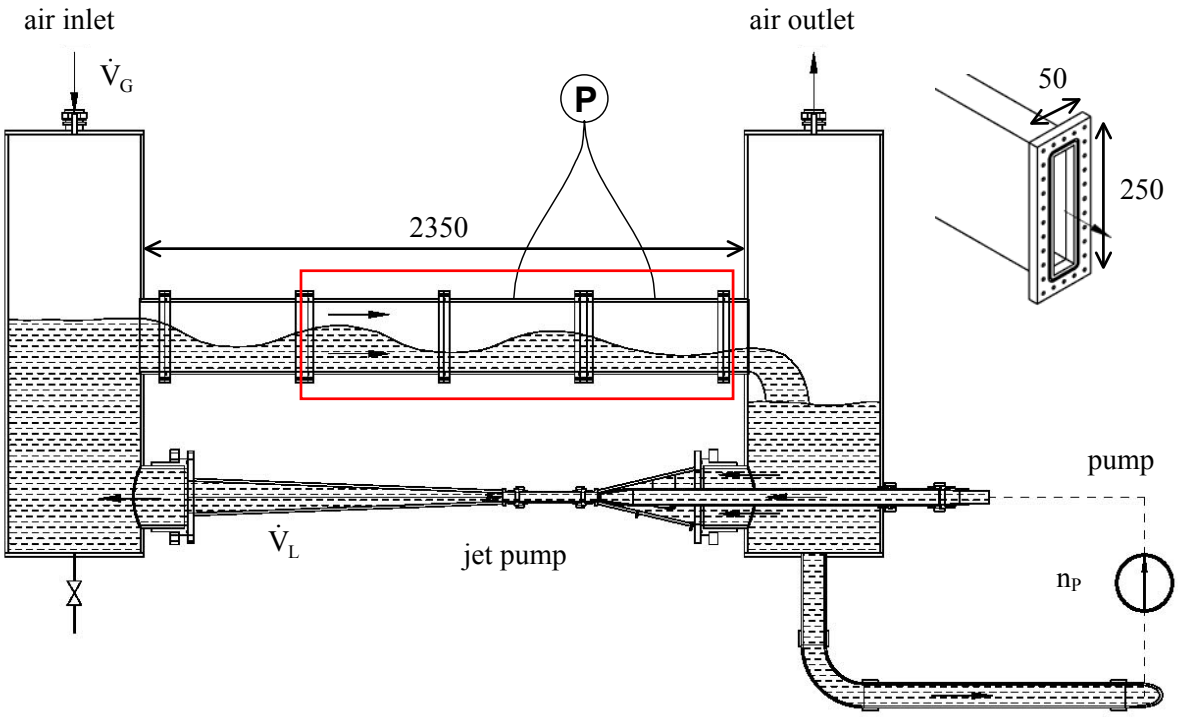

Fig. 2.1: Schematic view of the horizontal channel with inlet separator and modelled part (red)

In the following, a selected co-current test run is analysed. It was carried out at a superficial water velocity of 0.69 m/s and a superficial air velocity of 2.2 m/s. The pressure was ambient and the water temperature 16,5°C. Under these conditions, a slug flow is generated.

2.2 CFD model of the duct

The CFD calculation was performed using the software package *CFX-5.7* (*CFX*, 2004). The main characteristics of the solver are:

- Finite element based finite volume method for hybrid unstructured meshes;
- Coupled solver for momentum and mass;
- Implicit pressure based formulation;
- Co-located variables;
- Algebraic multi-grid method;
- High parallelisation;
- A selection of different time and space discretization schemes;

- Availability of different turbulence models (k-ε model, k-ω model, SST model, Reynolds stress models, LES with Smagorinsky subgrid model);
- Multi-phase formulations: Lagrangian particle tracking, homogenous multi-phase model, Euler-Euler multi-phase formulation (particle model, mixture model).

For slug flow simulations in horizontal pipes and channels, an appropriate multiphase flow model has to be selected in combination with the *CFX* free surface model. Due to the geometrical scale of the horizontal channel it is not possible to resolve the spatial structure of the free surface into the micro-scale with the CFD model. A slug flow simulation can therefore not cover onset and evolution of Kelvin-Helmholtz instabilities at the free surface. The interface drag law applied to the location of the free surface must consider the influence of these free surface instabilities on the macro-scale flow properties. Additionally, the movement of the free surface at the inlet boundary condition introduces instabilities.

For free surface simulations, the inhomogeneous multiphase model recommended by Frank (2003) was used, where the gaseous and liquid phases can be partially mixed in certain areas of the flow domain. In this case, the local phase demixing after gas entrainment is controlled by buoyancy and interphase drag and is not hindered by the phase interface separating the two fluids. A surface capturing method using a compressive advection scheme is used in *CFX*. Explicit interface tracking methods (e.g. VOF or Level Sets methods) were not applied. A further decision has to be made regarding the applied fluid morphology and interphase drag law for the multiphase flow. The total drag force D is most conveniently expressed in terms of the dimensionless drag coefficient C_D,

$$D = \frac{1}{2} \cdot \rho_{\alpha\beta} \cdot \left(U_\alpha - U_\beta\right)^2 \cdot A \cdot C_D \tag{1}$$

where ρ is the fluid density, $(U_\alpha - U_\beta)$ is the relative speed and A is the projected area of the body in flow direction. In (1), α describes the liquid phase and β the gaseous phase.

The fluid-dependent shear stress transport (SST) turbulence models (Menter, 2001) were selected for each phase. Damping of turbulent diffusion at the interface was not considered. The *k-ω* based SST model accounts for the transport of the turbulent shear stress and gives highly accurate predictions of the onset and the amount of flow separation under adverse pressure gradients. The SST model combines the advantages of the Wilcox (1994) and of the *k-ε* model.

To take buoyancy effects into account, a buoyancy production term was used in the turbulence model and was included in the *k*- and *ω*-equations for additional turbulence production and dissipation. If the full buoyancy model is being used, the buoyancy production term P_{kb} is modelled according to *CFX* (2004) as:

$$P_{kb} = -\frac{\mu_t}{\rho \cdot Pr_t} \cdot g \bullet \nabla\rho \tag{2}$$

where ρ is the density of the fluid, Pr_t the turbulent Prandtl number, μ_t the turbulent viscosity and g the gravity vector.

2.3 Geometry, grid generation and boundary conditions

Due to very high numerical efforts of transient slug flow simulations, the modelling of the complete test facility is not feasible. In order to keep computational time within acceptable limits, only the horizontal test section with its rectangular cross-section was modelled. The model dimensions are:

length x height x width = 2000 x 250 x 50 mm³. The grid was created with *CFX-MESHBUILD* and transferred to *CFX-5 PRE*. It consists of $4x10^5$ hexahedral elements (number of nodes: length x height x width = 400 x 100 x 10), which reduces the computational time and improves the quality of the mesh compared to tetrahedrons. Two different grid densities were studied.

At the inlet of the channel, air and water velocities are set to constant values over the part of the inlet cross-section that is occupied by each phase. In accordance to the initial water level, the inlet velocities were set to values that correspond to the gas and liquid flow rates measured during the experiment. These velocities were kept constant in time. The turbulent kinetic energy and dissipation rate at the inlet were set to the standard values of *CFX-5*. The level at the inlet was varied according to the time history of the liquid level measured by the high-speed camera at $z_f = 0.75$ m (Fig. 2.2). The outlet boundary condition has been applied to the cross section at the other end of the horizontal channel and was pressure controlled. The outer walls of the channel were set as hydraulically smooth walls with a non-slip boundary condition applied to both gaseous and liquid phases.

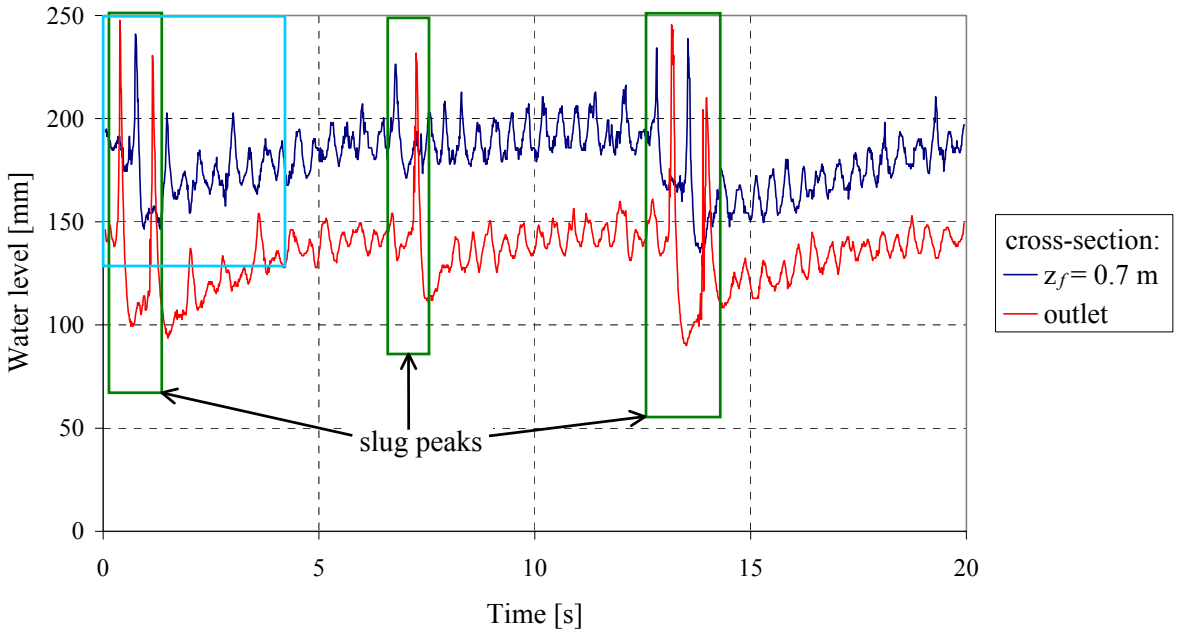

Fig. 2.2: Time-dependent water level by slug flow (100 Hz measurement)

2.4 Results

The picture sequence (see Fig. 2.3) shows the flow observed during the experiment in comparison to the corresponding CFD calculation. In both cases, a slug is developing. In the CFD calculation, the slug develops approximately at $t = 0.90$ s due to a high peak of the experimental water level at the inlet cross-section. The tail of the calculated slug and the flow behind it is in good agreement with the experiment. The entrainment of droplets in front of the slug could not be observed in the calculation. However, the rolling over and breaking of the wave, characteristic of a slug, are clearly to be seen in Fig. 2.3. These are created by the shear generated by the high air velocity.

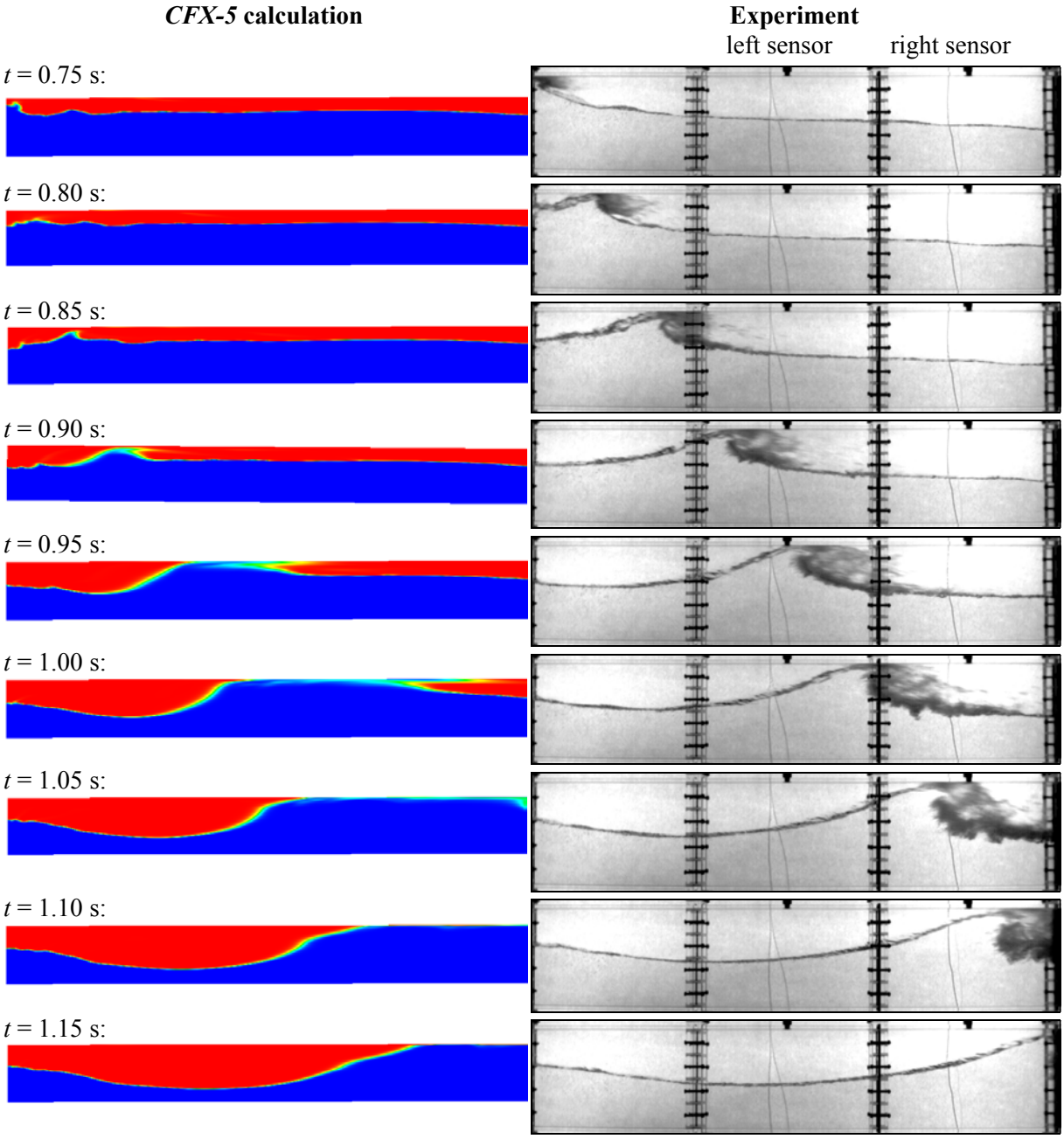

Fig. 2.3: Comparative picture sequence of the recalculated slug

In contrast to the measurement, the slug length is increasing in time in the calculation. This could be a result of the different amount of water in the channel at the beginning of the experiment and the simulation. While in the simulation, the liquid phase covered 78% of the channel, it represented about 70% at the beginning of the experiment. Furthermore, in the experiment, this value was also reduced by a first slug, which carried a significant amount of water out of the channel. This first slug could not be simulated. This is probably an effect of the simplified initial conditions assumed in the calculation. Because of the constant initial water level, it took quite a long simulation time to establish a wavy flow along the channel, which is necessary for slug formation. Whereas at the beginning of the measurements, the test channel was already in a fully established intermittent slugging regime.

The slug position extracted from the camera images is compared with the calculation result in Fig. 2.4. In the experiment, the slug moves along the duct with a constant velocity. The velocity of the slug selected for the post-test calculation was 3.7 m/s. In contrast to this, the calculated slug propagation is characterized by an acceleration phase between 0.75 and 0.90 s, when the slug is still in the process of formation. In a second phase, starting from $t = 0.90$ s, when the wave blocks the whole cross-section of the channel, the velocity of the calculated slug stays nearly constant at 4.4 m/s on average. This is 18% higher than the experimental value.

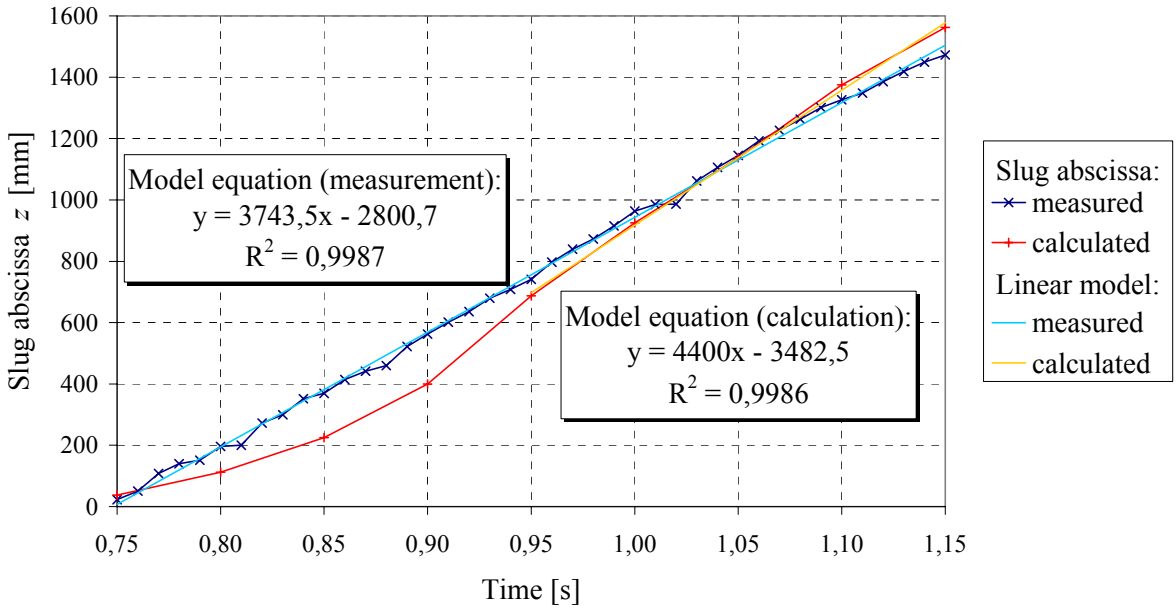

Fig. 2.4: Propagation of a slug - comparison between measurement and calculation

Fig. 2.5 shows the pressure field created by the slug in the CFD calculation. Due to the fact that the slug is driven by the gas pressure, a steep pressure gradient is observed at the slug front. This leads to the typical pressure history recorded by the transducers on top of the channel, which indicate a sudden pressure increase when the slug passes by (Fig. 2.6). Typical rise times are 2 ms (left sensor) and 10 ms (right sensor). The rise time is linked to the slug length: as the slug becomes longer between the two sensors, the time needed to pass the second sensor and, therefore, to reach the high-pressure level increases. The pressure decreases simultaneously on both sensor positions, when the slug reaches the outlet separator.

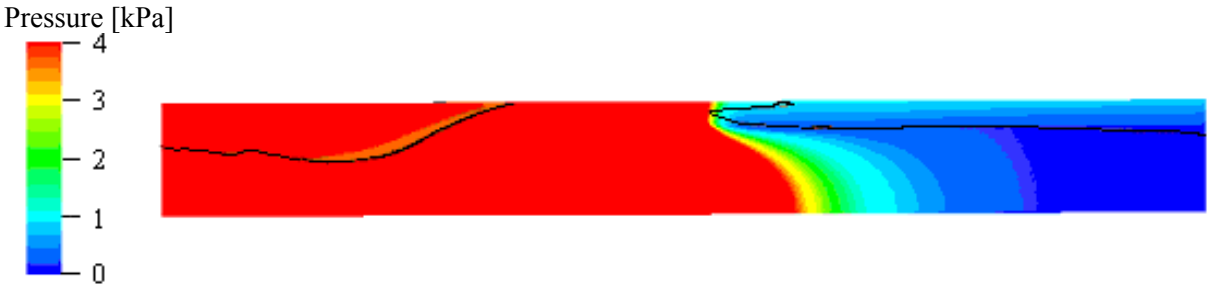

Fig. 2.5: Calculated pressure field at t *= 0.95 s*

The comparison of the time-dependent pressure at both sensor positions for the experiment and the calculation also shows that the first slug observed in the test was not simulated. Therefore, only the

second pressure increase can be compared with the calculation. In the simulation, the pressure at the first sensor position increases later than in the experiment. At the second sensor position the increase happens simultaneously. Then the pressure decreases earlier in the calculation than in the experiment. All this is a consequence of the differences in the slug propagation (see Fig. 2.4).

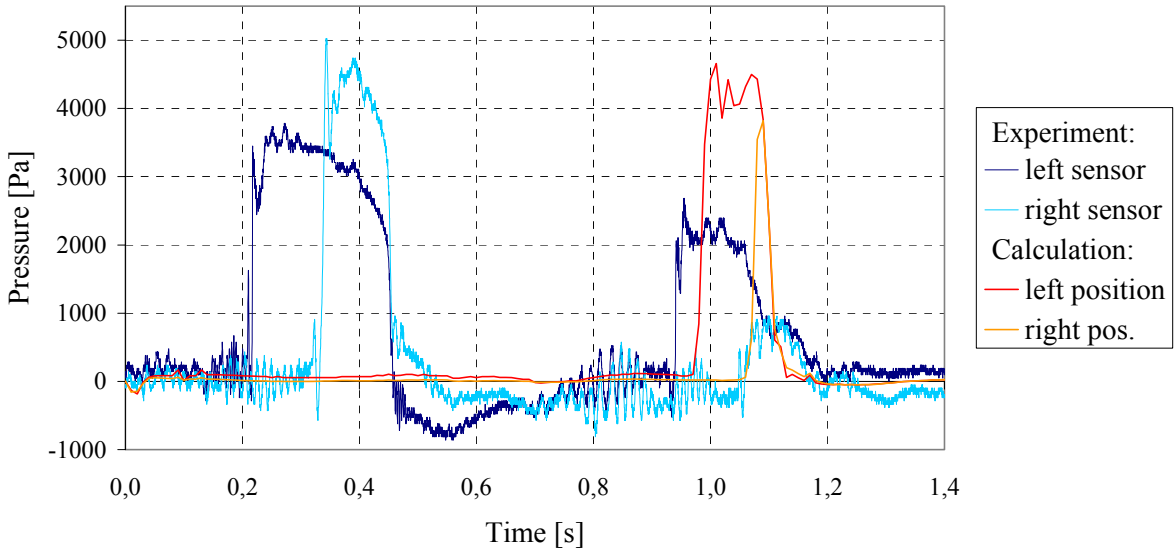

Fig. 2.6: Transient pressure at both sensor positions for experiment and CFX *calculation*

Furthermore, the calculation overestimated the peak pressure (4.4 kPa) in comparison to the experiment (2.3 kPa). This is due to the different size of the experimental slugs. Since, in the experiment, the first slug cleared a certain amount of water from the channel, the second slug is much smaller than the first one. That is why the peak pressure of the first slug reaches between 3.6 and 5.0 kPa (respectively at the first and second sensor positions), which is the order of magnitude of the calculated pressure peak.

2.5 Particle Image Velocimetry (PIV) of a slug

To show the velocity field inside the slug, a PIV-system was used. The laser-light sheet was focused in the middle of the test section. The PIV camera was directed to the upper part of the duct, in the region of the first pressure sensor.

A PIV picture of a slug with the calculated velocity field is shown in Fig. 2.7. The slug propagation velocity is approximately 3.8 m/s, which is close to the velocity of the slug analysed in the previous section. The vector colour shows that the small leak air flow on top of the slug entrains the water at local absolute velocities of about 6 m/s. The lengths and directions of the vectors show the velocities in a coordinate system that moves with the slug propagation velocity. It reveals the structure of the flow circulation inside the slug.

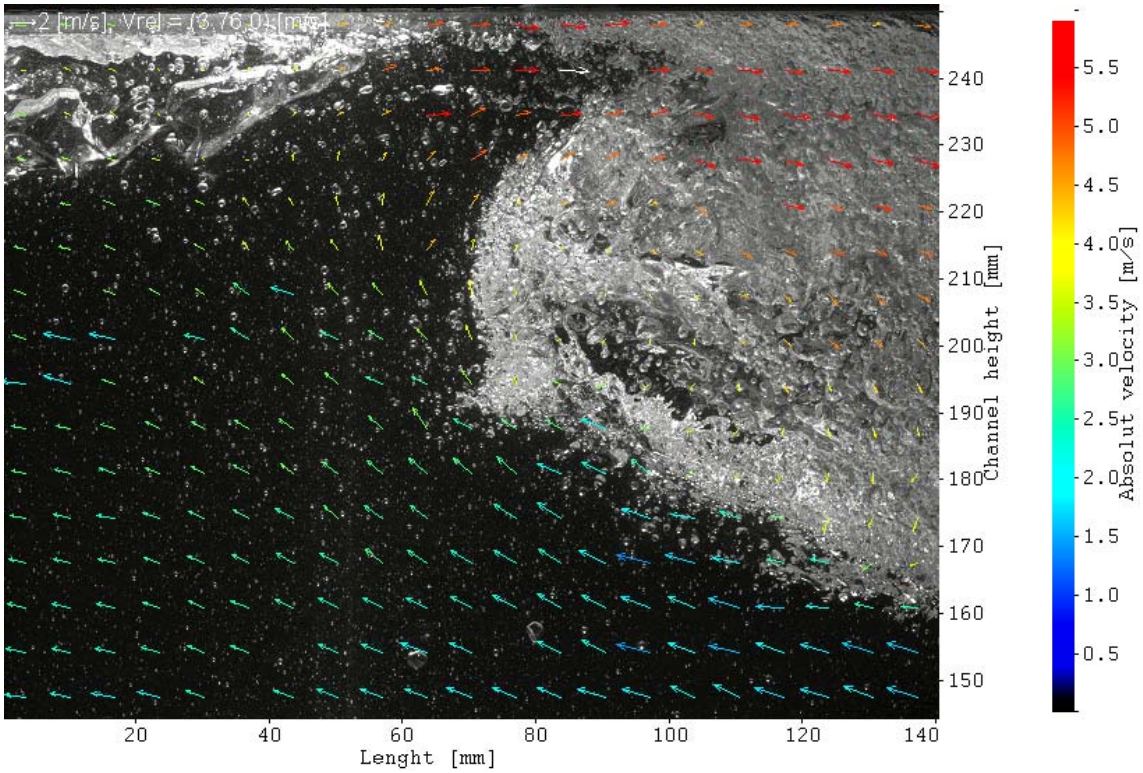

Fig. 2.7: Velocity field inside a slug (the vector colour shows the absolute velocity, its length and direction show the relative velocity compared to the propagation velocity of the slug)

2.6 Conclusions

This preliminary study shows that the slug flow regime can be qualitatively reproduced with CFD. In order to perform reasonable quantitative comparisons, the experimental boundary conditions at the inlet have to be constant and well defined. Because of the separator at the test-section inlet, important inlet parameters such as water level and velocity profiles cannot be controlled properly and are not stationary in the present facility. Therefore, detailed investigations require an improved inlet geometry. This was realised in a new test facility, which is described in section 3.

3. CFD model for a self-generation of slug flow

3.1 The horizontal channel with separate injection of water and air into the test-section

The Horizontal Air/Water Channel (HAWAC) (Fig. 3.1) is devoted to co-current flow experiments. A special inlet device provides defined inlet boundary conditions by a separate injection of water and air into the test-section. A blade separating the phases can be moved up and down to control the free inlet cross-section for each phase. This allows to influence the evolution of the two-phase flow regime. The cross-section of this channel is smaller than the previous one (described in section 2): its dimensions are 100 x 30 mm² (height x width). Thus it fits the field of view of the PIV-system and makes it possible to cover a wider range of superficial velocities. The test-section is about 8 m long, and therefore the length-to-height ratio L/h is 80. Alternatively, related to the hydraulic diameter, the dimensionless length of the channel is $L/D_h = 173$.

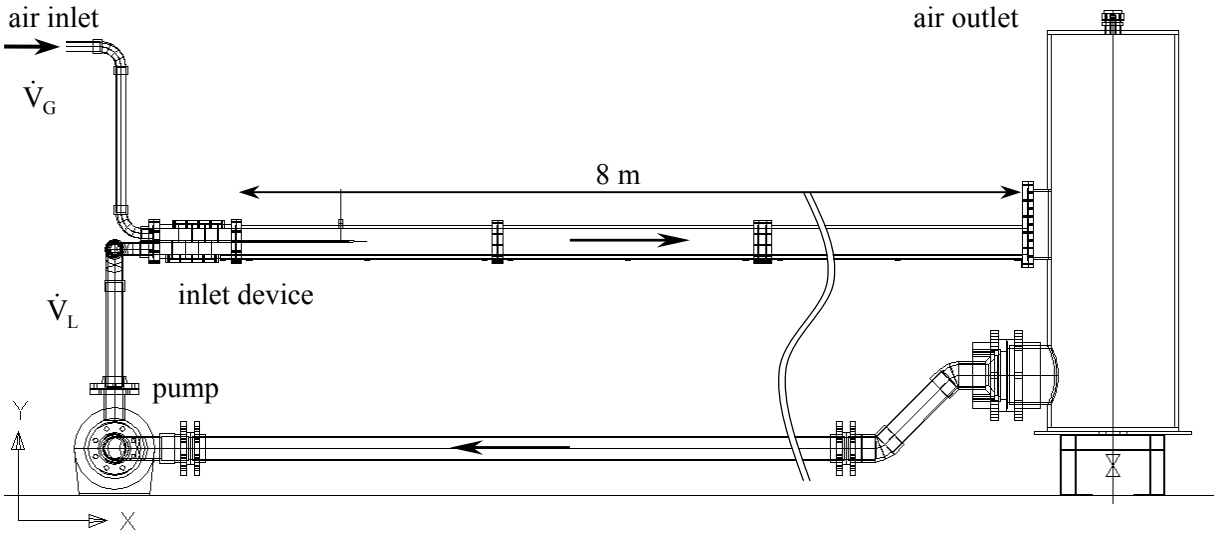

Fig. 3.1: Schematic view of the horizontal channel with inlet device for a separate injection of water and air into the test-section

The inlet device (Fig. 3.2) is designed for a separate injection of water and air into the channel. The air flows through the upper part and the water through the lower part of this device. Because the inlet geometry produces a lot of perturbations in the flow (bends, transition from pipes to rectangular cross-section), 4 wire mesh filters are mounted in each part of the inlet device. The filters are made of stainless steel wires with a diameter of 0.63 mm and have a mesh size of 1.06 mm. They aim at providing homogenous velocity profiles at the test-section inlet. Moreover, the filters produce a pressure drop that attenuate the effect of the pressure surge created by slug flow on the fluid supply systems.

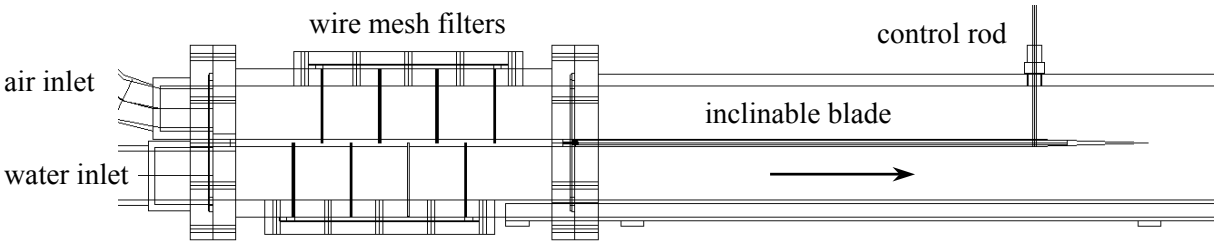

Fig. 3.2: The inlet device

Air and water come in contact at the final edge of a 500 mm long blade that divides both phases downstream of the filter segment. The free inlet cross-section for each phase can be controlled by inclining this blade up and down. In this way, the perturbation caused by the first contact between gas and liquid can be either minimised or, if required, a perturbation can be introduced (e. g. an hydraulic jump). Both, filters and inclinable blade, provide well-defined inlet boundary conditions for the CFD model and therefore offer very good validation possibilities. Optical measurements were performed with a high-speed video camera.

3.2 Flow pattern map of the HAWAC

A flow pattern map (Fig. 3.3) was arranged constructed on the basis of a visual observation of the flow structure at different combinations of the gas and liquid superficial velocities. The maximum superficial velocities achieved in the test-section are 2 m/s for the water and 8 m/s for the air. The observed flow patterns are:

1 stratified flow
2 wavy flow
3 elongated bubble flow
4 slug flow
5 droplet/film flow (equivalent to annular flow in pipes)

Further, sub-categories were defined to consider the slug generation frequency and the appearance of elongated bubbles:

a sporadic (transition regime)
b periodic, but only one type of structure (either slug or elongated bubble)
c periodic and several types of structure simultaneously

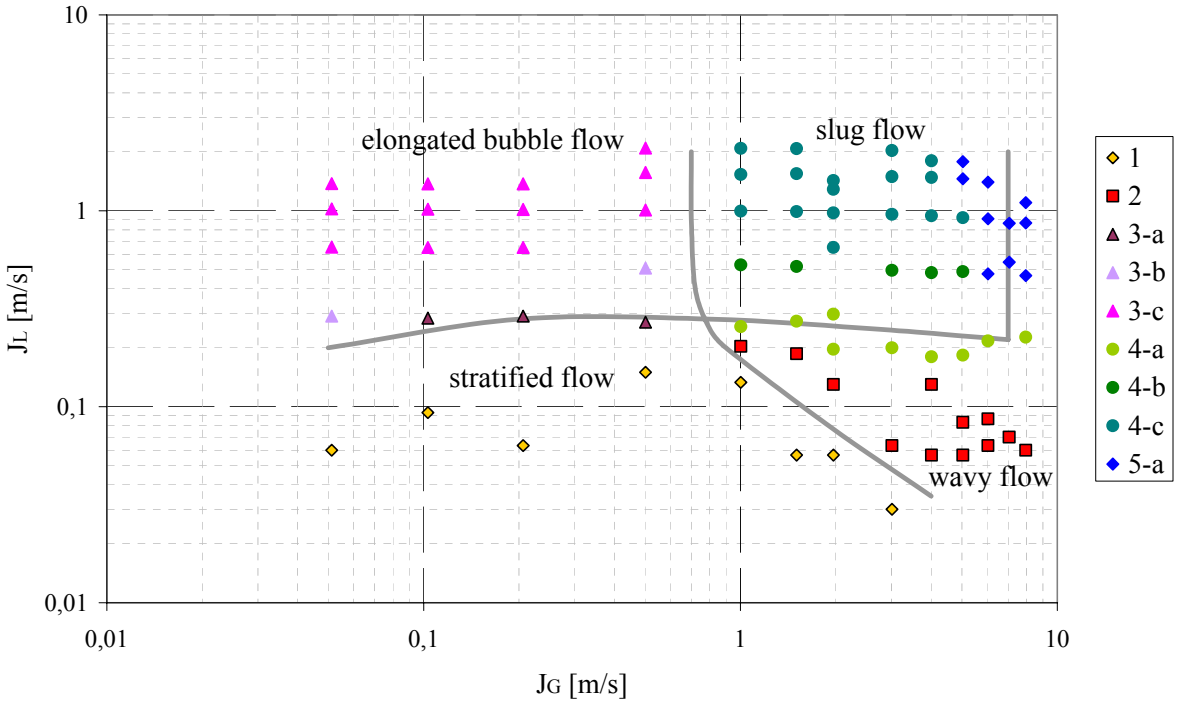

Fig. 3.3: Flow pattern map for the rectangular channel (inlet blade in horizontal position)

It was observed that the position of the inlet blade not always defines the water level at the inlet. For example at very low water flow rates, the water flow separates from the lower surface of the blade and the initial water level is lower than the height of the outlet edge of the blade. The corresponding test points are marked in the flow map by a black border. To create proper inlet boundary conditions at these flow rates, the blade has to be inclined down.

The observations were repeated with an inclined blade (upwards and downwards). These tests have shown that the inclination of the blade can have an important influence on the evolution of the flow regime along the test-section. For example, the inlet length needed for slug generation can vary from 0.5 to 3 m just by changing the blade position from an opening ration of 20/80 (air/water) to 80/20. Nevertheless, and despite a short channel length, the flow regime established at the end of the channel is not significantly affected by the plate inclination.

In the flow map, some transitions are different from those found by Mandhane (1974) and Baker (1954). Especially the transitions from stratified to elongated bubble flow and from wavy to slug flow were observed at higher liquid superficial velocities than in the literature. This can be attributed to the shorter channel length and would indicate that the flow regime is not fully established at the end of the test-section. In the future it is planned to prolong the channel by another 6 m, which will allow to study this effect in more detail.

3.3 CFD model of the duct, turbulence modelling in the interfacial area and boundary conditions

The second channel with rectangular cross-section was modelled using *ANSYS CFX*. The model dimensions are 4000 x 100 x 30 mm³ (length x height x width), which corresponds only to the first half of the test-section (Fig. 3.4-a). The grid consists of 6×10^5 hexahedral elements.

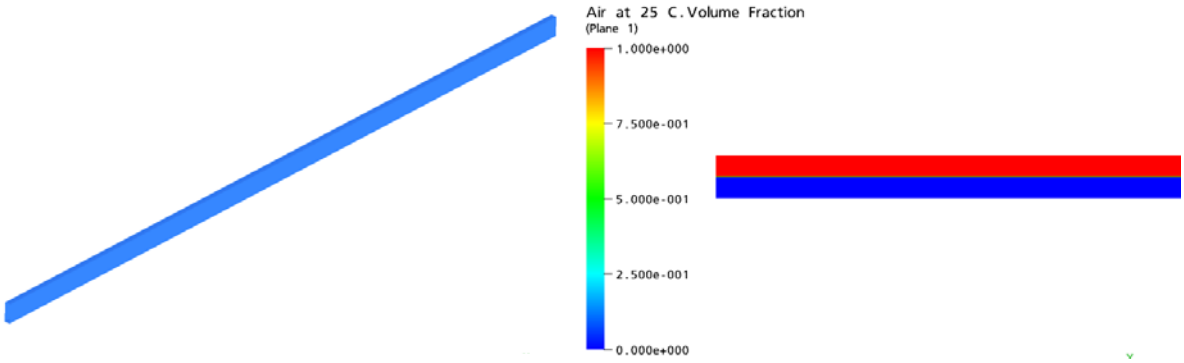

a) Fluid domain (channel) *b) Air volume fraction, initial state (Zoom) [-]*

Fig. 3.4: Model and initial conditions of the mass fractions

The slug flow experiment at a superficial water velocity of 1.0 m/s and a superficial air velocity of 5.0 m/s was chosen for the CFD calculations. In the experiment, the inlet blade was in horizontal position. Accordingly, the model inlet was divided into two parts: in the lower 50% of the inlet cross-section, water was injected and in the upper 50% air. An initial water level of $y_0 = 50$ mm was assumed for the entire model length (Fig. 3.4-b).

In the simulation, both phases have been treated as isothermal and incompressible, at 25°C and at a reference pressure of 1 bar. A hydrostatic pressure was assumed for the liquid phase. Buoyancy effects between the two phases are taken into account by the directed gravity term. At the inlet, the turbulence properties were set using the “Medium intensity and Eddy viscosity ratio” option of the

flow solver. This is equivalent to a turbulence intensity of 5% in both phases. The inner surface of the channel walls has been defined as hydraulically smooth with a non-slip boundary condition applied to both gaseous and liquid phases. The channel outlet was modelled with a pressure controlled outlet boundary condition.

As the goal of the CFD calculation was to induce surface instabilities, which are later generating waves and slugs, the interfacial momentum exchange and also the turbulence parameters had to be modelled correctly. Without any special treatment of the free surface, the high velocity gradients at the free surface, especially in the gaseous phase, generate too high turbulence throughout the two-phase flow when using the differential eddy viscosity models like the k-ε or the k-ω model (*ANSYS CFX*, 2005). Therefore, certain damping of turbulence is necessary in the interfacial area because the mesh is too coarse to resolve the velocity gradient in the gas at the interface. On the gas side of the smooth free surface, this damping should be similar to that used near a solid wall. Moreover, on the liquid side the advanced model should take the anisotropy between the normal and the tangential Reynolds stresses into account. A simple symmetric damping procedure provides for the solid wall-like damping of turbulence in both gas and liquid phases. Therefore, a damping of turbulent diffusion at the interface was applied in this calculation by an appropriate source term in the ω-equation:

$$A \cdot \Delta y \cdot \beta \cdot \rho_i \cdot \left(B \cdot \frac{6 \cdot \mu_i}{\beta \cdot \rho_i \cdot \Delta n^2} \right)^2 \tag{3}$$

where A the interface area density, Δn is the typical grid cell size across the interface, ρ_i and μ_i are the density and viscosity of the phase i. Further, the model parameter B should have a value of 100.

The parallel transient calculation of 5.0 s of simulation time on 4 processors last 4 days. A high-resolution discretization scheme was used. For time integration, the fully implicit second order backward Euler method was applied with a constant time step of $dt = 0.001$ s and a maximum of 15 coefficient loops. A convergence in terms of the RMS values of the residuals to be less then 10^{-4} could be assured most of the time.

3.4 Results

In the following picture sequences (Fig. 3.5 and 3.6) a comparison is presented between CFD calculation and experiment: the calculated phase distribution is visualized and comparable camera frames are shown. In both cases, a slug is generated. The sequences show that the qualitative behaviour of the creation and propagation of the slug is similar in the experiment and in the calculation. In the CFD calculation, the slug develops at approximately $t = 1.30$ s, induced by instabilities. The single effects leading to slug flow that can be simulated are shown in details in Fig. 3.7. These phenomena are:

- Instabilities and small waves are generated by the interfacial momentum transfer randomly (Fig. 3.7-a). As a result bigger waves are generated.
- The waves can have different velocities and can merge together (Fig. 3.7-b and c).
- Bigger waves roll over (Fig. 3.7-c) and can close the channel cross-section (Fig. 3.7-d).

The needed entrance length for slug generation was defined as the length between the inlet and there a wave closes nearly the entire cross-section for the first time. This was observed at about 1.5 m in the experiment and 2.5 m in the calculation.

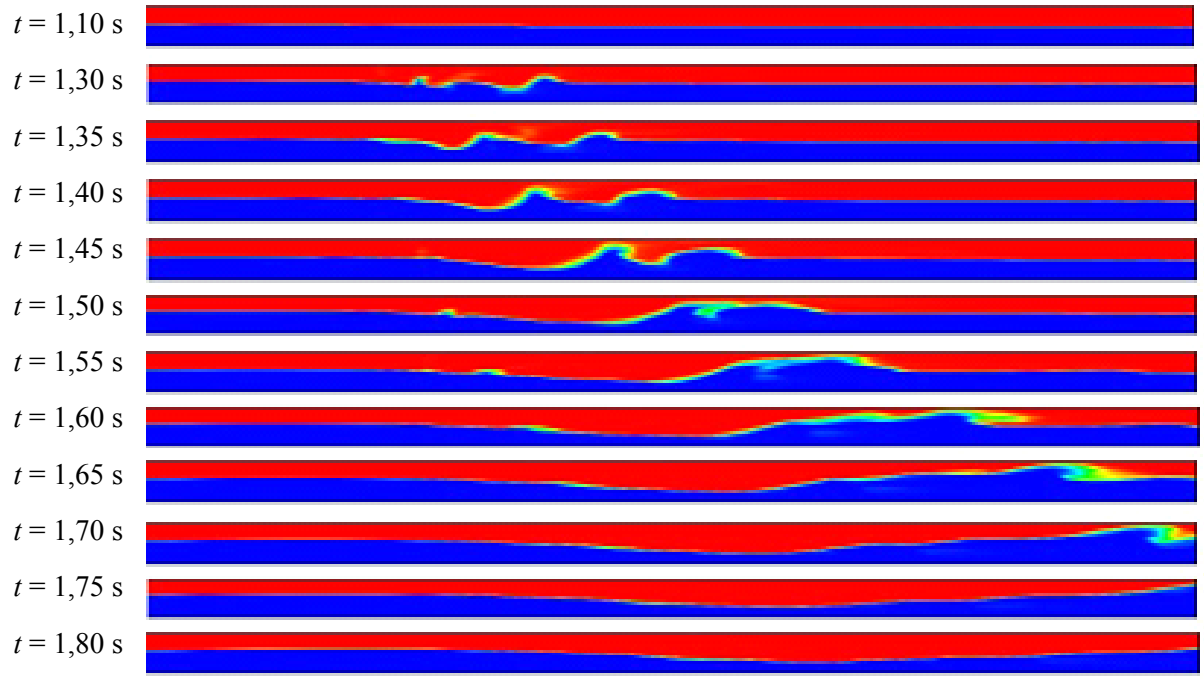

Fig. 3.5: Calculated picture sequence at J_L = 1.0 m/s and J_G = 5.0 m/s (depicted part of the channel: 1.4 to 4 m after the inlet)

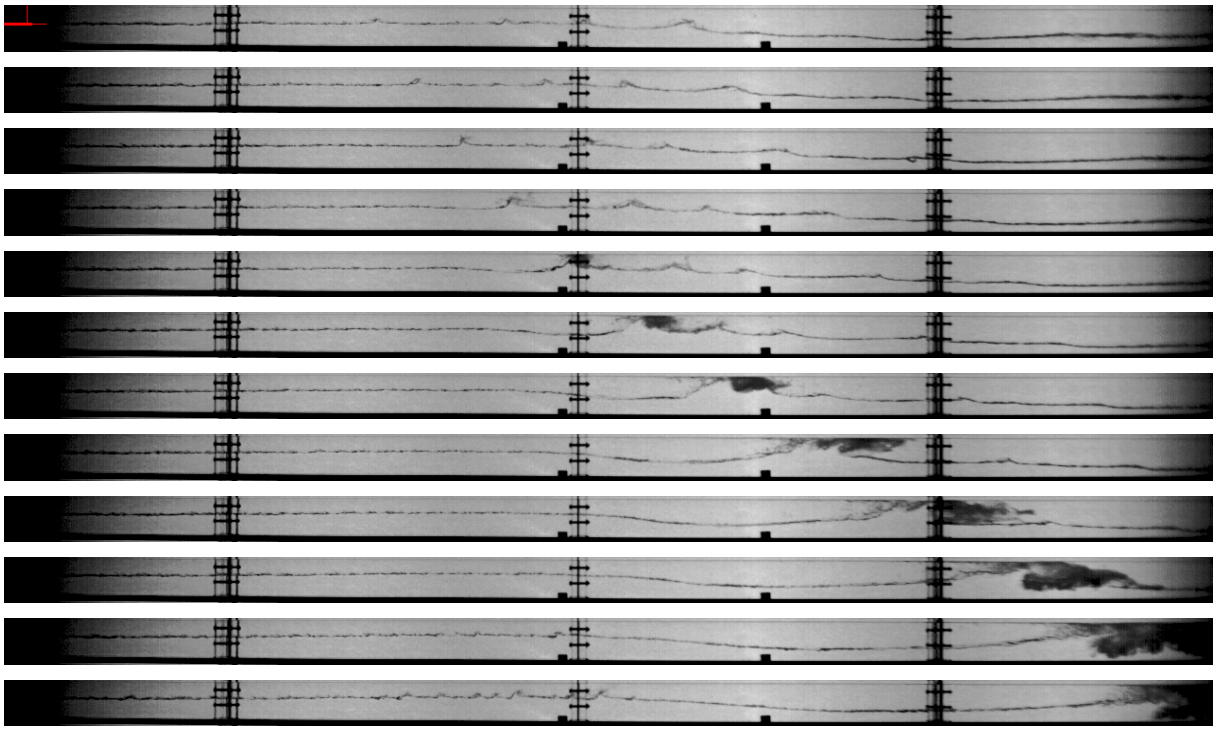

Fig. 3.6: Measured picture sequence at J_L = 1.0 m/s and J_G = 5.0 m/s with Δt = 50 ms (depicted part of the channel: 0 to 3.2 m after the inlet)

In contrast to the measurement, the stratified flow after the slug calculated with *ANSYS CFX* is too smooth, which defers the generation of the next slug. Since the slug cleared an important amount of water from the channel, the next slug appears after the channel is slowly filled up again by the

transport of liquid from the inlet. This process takes approximately 1.5 s. In the experiment, small waves are generated immediately after the slug and create the next one within 0.3 to maximum 0.7 s. Sources of instabilities are here the high air velocity but also the pressure surge created by the slugs, particularly when they leave the channel. This effect has not been proper simulated since just the half of the channel was modelled. Therefore, the slug frequency cannot be compared at this stage of the simulation.

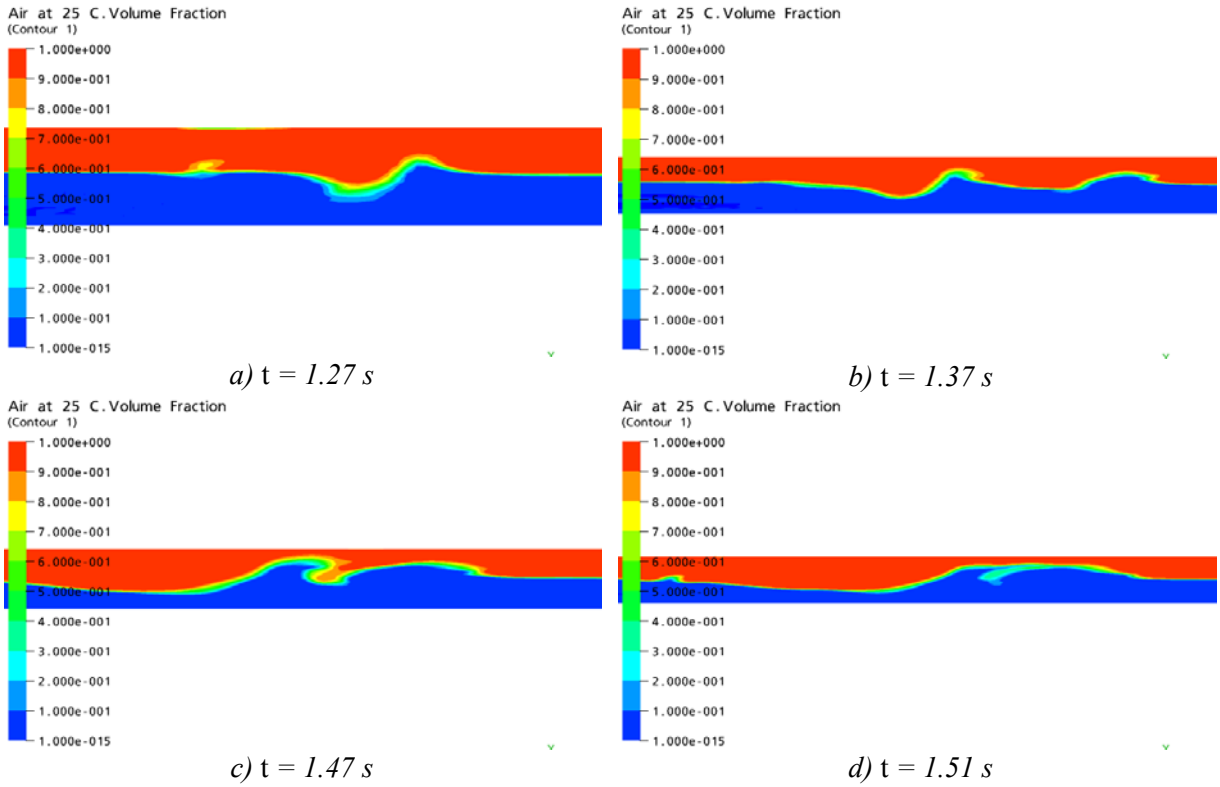

a) t = *1.27 s* *b)* t = *1.37 s*

c) t = *1.47 s* *d)* t = *1.51 s*

Fig. 3.7: Details of the slug generation calculated with ANSYS CFX *at different simulation time*

Summary and conclusions

For the investigation of an air/water slug flow, two horizontal channels with rectangular cross-section were built at *Forschungszentrum Rossendorf*. In the first channel with a separator at the inlet, optical measurements were performed with a high-speed video camera and were complemented by simultaneous dynamic pressure measurements. By an interface capture method, the water level history can be extracted from the image sequences. Furthermore, the velocity field of a slug was measured using Particle Image Velocimetry (PIV). It reveals the inner flow circulation of the slug, around the point there the slug is rolling over. A CFD simulation of stratified co-current flow was performed using the code *CFX-5.7* applying the two-fluid model with the free surface option. No explicit interface tracking methods (e.g. VOF or Level Sets methods) were used. Slug flow was successfully simulated with a transient simulation, using a time-dependent inlet water level from the experimental data.

In the HAWAC test facility, a special inlet device provides well defined as well as variable boundary conditions, which allow very good CFD-code validation possibilities. A flow pattern map was arranged and shows the potential of the facility. A picture sequence recorded during slug flow was compared with the equivalent CFD simulation made with the code *ANSYS CFX*. The two-fluid model

was applied with a special free surface treatment. Due to an interfacial momentum transfer, it was possible to generate slugs based on instabilities. The behaviour of slug generation and propagation at the experimental setup was qualitatively reproduced, while deviations require a continuation of the work. The creation of small instabilities due to pressure surge or an increase of interfacial momentum should be analysed in the future. Furthermore, experiments like pressure and velocity measurements are planned and will allow quantitative comparisons, also at other superficial velocities.

Acknowledgements

This work is carried out in the frame of a current research project funded by the German Federal Ministry of Economics and Labour, project number 150 1265.

References

Anglart, H., and Podowski, M. Z. 2002. Fluid mechanics of Taylor bubbles and slug flows in vertical channels. Nuclear science and engineering, 140, 165-171.

ANSYS CFX 2005. User Manual. ANSYS Inc.

Baker, O. 1954. Simultaneous flow of oil and gas. Oil & Gas Journal, 53, 184-195.

Cook, M., and Behnia, M. 2001. Bubble motion during inclined intermittent flow. Int. J. of Heat and Fluid Flow, 22, 543-551.

Frank, T. 2003. Numerical simulations of multiphase flows using CFX-5. CFX Users conference, Garmisch-Partenkirchen, Germany.

Hope, C. B. 1990. The development of a water soluble photocromic dye tracing technique and its application to two-phase flow. PhD thesis, Imperial College of Science, Technology and Medicine, London.

Ishii M. 1990. Two-fluid model for two-phase flow. Multiphase Science and Technology, 5, Edited by G. F. Hewitt, J. M. Delhaye, N. Zuber, Hemisphere Publishing Corporation, 1-64.

Issa, R. I., and Tang, I. F. 1990. Modelling of vertical gas-liquid slug flow in pipes. Proc. Symp. On Advances in Gas-Liquid flows, Dallas.

Lun, I., Calay, R. K., and Holdo, A. E. 1996. Modelling two-phase flows using CFD. Applied Energy, 53, 299-314.

Manfield, P. D. 2000. Experimental, computational and analytical studies of slug flow. PhD thesis, Imperial College of Science, Technology and Medicine, London.

Mandhane, J. M., Gregory, G. A., and Aziz, K. 1974. A flow pattern map for gas-liquid flow in horizontal pipes: predictive models," Int. J. Multiphase Flow, 1, 537-553.

Mao, Z., and Dukler, A. E. 1991. The motion of Taylor bubbles in vertical tubes. II. Experimental data and simulations for laminar and turbulent flow. Chem. Eng. Sci., 46, 2055-2075.

Menter, F. R. 1993. Zonal two-equation k-ω turbulence models for aerodynamic flows. AIAA, 93-2906.

Menter, F. R. 2002. CFD best practice guidelines for CFD code validation for reactor safety applications. EC project ECORA, report EVOL-ECORA-D01.

Moe, R. 1992. Transient simulation of 2-3D stratified and intermittent two-phase flows. PhD thesis, University of Oslo.

Odozi, U. A. 2000. Three-phase gas/liquid/liquid/ slug flow. PhD thesis, Imperial College of Science, Technology and Medicine, London.

Pan, L. 1996. High pressure three phase (gas/liquid/liquid) flow. PhD thesis, Imperial College of Science, Technology and Medicine, London.

Scheuerer, M. 2003. Selection of PTS-relevant test cases, EC-report EVOL-ECORA D05a.

Soleimani, A., and Hanratty, T. J. 2003. Critical liquid flows for the transition from the pseudo-slug and stratified patterns to slug flow. Int. J. of Multiphase Flow, 29, 51-67.

Sühnel T. 2003. Aufbau und Inbetriebnahme eines horizontalen Luft-Wasser-Strömungskanals. Diplomarbeit, Institut für Sicherheitsforschung, FZ Rossendorf, Dresden.

Ubbink O. 1997. Numerical prediction of two fluid systems with sharp interfaces. PhD thesis, Imperial College of Science, Technology and Medicine, London.

Ujang P. M. 2003. A three-dimensional study of Taylor bubble turning in two-phase down flow. Second MIT conference on computational fluid and solids mechanics, Elsevier Science Ltd., Ed.: K.J. Bathe, 1176-1180.

Vallée, C., Höhne, T., Prasser, H.-M., Sühnel, T. 2005, Experimental modelling and CFD simulation of air/water flow in a horizontal channel. International topical meeting NURETH-11, Avignon, France, log# 479.

Wilcox, D. C. 1994. Turbulence modelling for CFD. La Cañada, California: DCW Industries Inc.

Woods, B. D., and Hanratty, T. J. 1999. Influence of Froude number on physical processes determining frequency of slugging in horizontal gas-liquid flows. Int. J. of Multiphase Flow, 25, 1195-1223.